Results of bedrock mapping in the Gemmell Lake area, Lynn Lake greenstone belt, northwestern Manitoba (Parts of NTS 64C11, 14): Implications for Au exploration

by Xue-Ming (Eric) Yang

Manitoba Geological Survey, 360-1395 Ellice Avenue, Winnipeg, MB R3G 3P2, Canada

(presented at Central Canada Mineral Exploration Convention, November 18-19, 2019, Winnipeg)

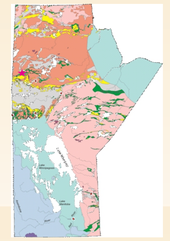

Abstract

Bedrock mapping at 1:20 000 scale in the 2019 summer was focused on the Gemmell Lake area in southern supracrustal belt of the Paleoproterozoic Lynn Lake greenstone belt. This aims to resolve the key questions about the relationship of Au mineralization to structures, hostrocks, granitoid intrusions and tectonic evolution, and to support ongoing exploration activity. The results indicate that the area is underlain by the Wasekwan group supracrustal rocks, comprising massive to pillowed basalt, basaltic andesite, dacite to rhyolite and related volcaniclastic rocks, and subordinate sedimentary rocks. The volcanic sequence is associated with reworked volcaniclastic and epiclastic rocks, suggestive of deposition in a setting comparable to volcanic arcs or back-arc basins. Unconformably overlying the Wasekwan group are the Sickle group sandstone and polymictic conglomerate, which are interpreted to have formed in localized synorogenic basin(s). A set of intrusions divided into pre-Sickle, post-Sickle and late intrusive suites cuts the supracrustal rocks, which were subjected to multiple phases (D_1 to D_6) of deformation and metamorphism.

Two styles of Au mineralization are evident in the Gemmell Lake area: 1) Au-bearing mylonite and silicified-sericitized (±disseminated arsenopyrite, pyrite) felsic volcanic to volcaniclastic rocks controlled by the Johnson shear zone, which is related to D_2 deformation and intersected by D_3 faults and associated structures; and 2) intrusion-hosted Au-bearing quartz (±carbonate, sulphide) vein systems controlled by intersections of D_3 faults and the D_2 Johnson shear zone. The field relationships suggest that timing of the Au mineralization was syn- to post-D_2 deformation. The D_2 event postdated the pre-Sickle intrusions, postdated or was contemporaneous with the post-Sickle intrusive suites, and predated the late intrusive suite. The post-Sickle adakite-like quartz diorite intrusions (subunit 7a) were likely emplaced in a post-subduction extensional setting resulting from the upwelling of asthenosphere mantle due to the rollback of the subducting slab. This was accompanied by anomalous heating that may have triggered the upward migration of auriferous fluids from the lower crust or upper lithosphere mantle along deep fault(s) connecting to the Johnson shear zone and associated structures in the middle to upper crust, consequently concentrating Au mineralization in favourable sites (e.g., chemical-structural traps).

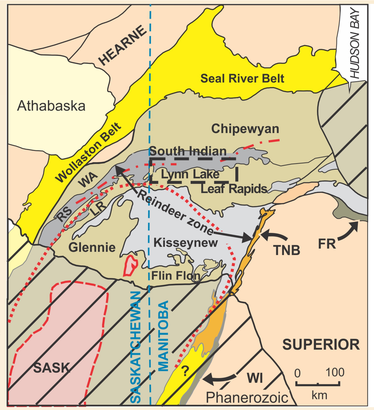

Fig. 1 Tectonic elements of the Trans-Hudson orogen in Manitoba and northeastern Saskatchewan, showing the major lithotectonic domains of the internal (Reindeer) zone of the Trans-Hudson orogen, Archean cratons and their Paleoproterozoic cover (external zones; after Zwanzig and Bailes, 2010).

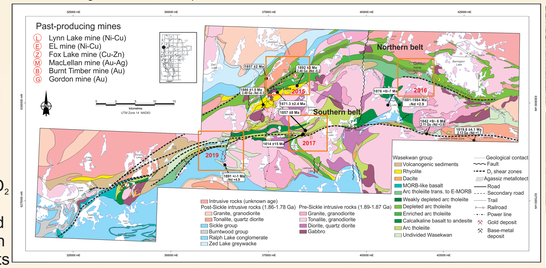

Fig. 2 Regional geology map of the Lynn Lake greenstone belt, showing detailed mapping areas in 2019 as well as in the past few field seasons (Yang, 2019a and references therein).

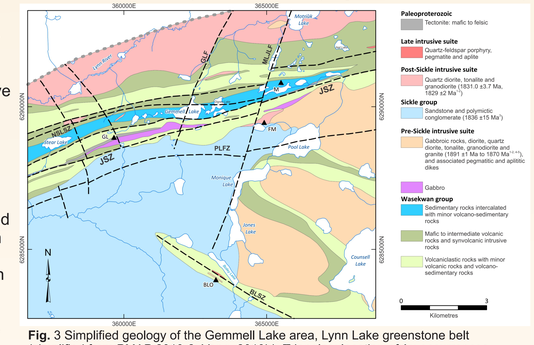

Fig. 3 Simplified geology of the Gemmell Lake area, Lynn Lake greenstone belt (simplified from PMAP 2019-2; Yang, 2019b). Triangles: location of Au occurrences.

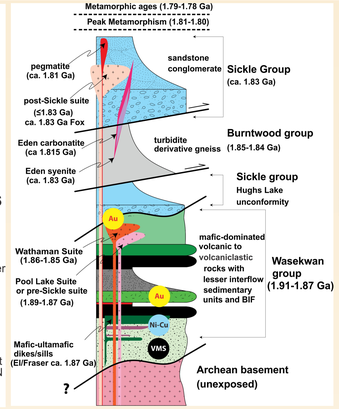

Fig. 4 Stratigraphic column of the Lynn Lake greenstone belt (modified from Lawley et al., 2019).

Field photographs of map units 1 to 9 rocks

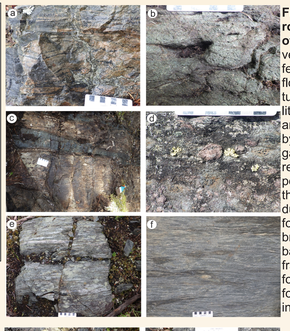

Fig. 5 Unit 1 volcaniclastic rocks with minor volcanics of the Wasekwan group: **a)** very fine grained quartz- and feldspar-phyric rhyolite with flow bands; **b)** intermediate tuff to lapilli tuff with rare lithic fragments; **c)** laminated andesitic tuff to lapilli tuff cut by a diabase dike); **d)** garnet-biotite schist with reddish garnet porphyroblasts, up to 2 cm, that are rotated clockwise due to dextral shear along S_2 foliation; e) foliated mafic tuff breccia and breccia with basaltic to andesitic fragments transposed by S_2 foliation; f) very strongly foliated basaltic tuff breccia in high-strain zone.

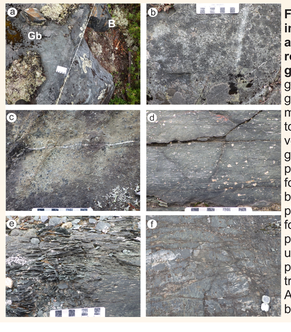

Fig. 6 Unit 2 mafic to intermediate volcanic rocks and synvolcanic intrusive rocks of the Wasekwan group: **a)** synvolcanic, massive gabbro (dike) cuts very fine grained aphyric basalt; **b)** massive gabbro with subhedral to euhedral plagioclase laths in very fine grained mafic groundmass; **c)** amphibole-phyric basaltic andesite; **d)** foliated plagioclase-phyric basalt; **e)** strongly foliated plagioclase-phyric basalt; **f)** foliated pillow basalt with well-preserved hyaloclastite selvage up to 3 cm thick; the stretched pillows are aligned along east-trending S_2 foliation planes. Abbreviations: Gb, gabbro; B, basalt.

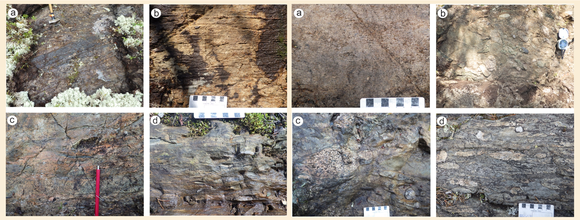

Fig. 7 Unit 3 sedimentary rocks intercalated with minor volcano-sedimentary rocks of the Wasekwan group: **a)** fine- to medium-grained, foliated quartzofeldspathic greywacke with alternating felsic and mafic bands or layering; **b)** laminated volcanic (andesitic) sandstone with biotite flakes and plagioclase clasts (0.5–2 mm) that have diffuse margins; **c)** volcanic sandstone containing disseminated magnetite, as well as magnetite aggregates up to 10 cm in length; **d)** volcanic breccia with felsic and mafic volcanic fragments in a felsic to intermediate sandy matrix; bedding transposed by S_2 foliation.

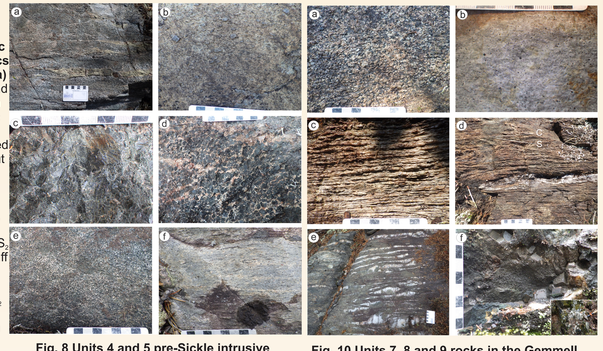

Fig. 8 Units 4 and 5 pre-Sickle intrusive suite: **a)** foliated, massive, medium- to coarse-grained equigranular gabbro with epidote veinlets and veins up to 4 cm wide present along S2 planes (unit 4); **b)** foliated, medium- to coarse-grained porphyritic granodiorite with quartz phenocrysts (2–5 mm; subunit 5a); **c)** megacrystic pyroxenite to melagabbro and d) massive, very coarse grained pyroxenite to melagabbro with cumulate texture (subunit 5b); **e)** massive, fine- to medium-grained quartz diorite (subunit 5b); and **f)** foliated, porphyritic muscovite-bearing granite (subunit 5c) with K-feldspar and quartz phenocrysts in felsic groundmass consisting of quartz, feldspar, biotite and muscovite, intruding unit 1 volcaniclastic and volcanic sedimentary rocks.

Acknowledgments

I thank M. Kohli for enthusiastic and capable field assistance and E. Anderson for logistical support. Thanks go to Alamos Gold Inc. for providing detailed airborne geophysical data. Thanks also go to L. Chackowsky for technical supports; M. Pacey for assembling the digital database for a hand-held data acquisition system; and C. Epp for cataloguing, processing and preparing the samples.

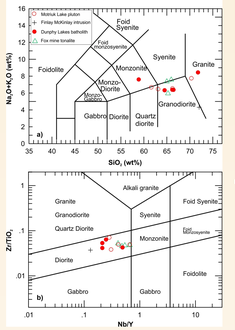

Fig. 11 Plots of total alkalis vs. SiO_2 (wt%) (a; Le Bas et al., 1986) and Zr/TiO_2 vs. Nb/Y (b; Pearce, 1996) for whole-rock samples for unit 7 and other ~1.3 Ga intrusions.

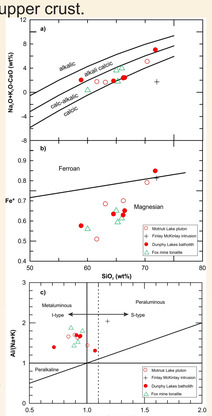

Fig. 12 Geochemical discrimination diagrams: **a)** plot of MOLI vs. SiO_2; **b)** Fe* vs. SiO_2 (after Frost et al., 2001); **c)** molar Al/(N+K) vs. Al/(Ca+Na+K) (Maniar and Piccoli, 1989). Boundary between I- and S-type granites is based on ANCK value of 1.1 (Chappell and White, 1974).

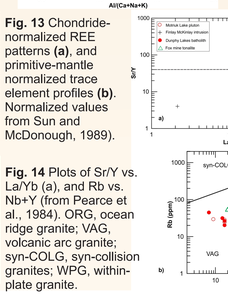

Fig. 13 Chondrite-normalized REE patterns **(a)**, and primitive-mantle normalized trace element profiles **(b)**. Normalized values from Sun and McDonough, 1989).

Fig. 14 Plots of Sr/Y vs. La/Yb (a), and Rb vs. Nb+Y (from Pearce et al., 1984). ORG, ocean ridge granite; VAG, volcanic arc granite; syn-COLG, syn-collision granites; WPG, within-plate granite.

Geochemical characteristics of adakite-like quartz diorites of unit 7 in post-Sickle intrusive suite

Figs. 11 to 14 indicate that the following key points for unit 7 quartz diorites in the post-Sickle intrusive suite.

1) They are dominantly calc-alkaline, and spread a range of lithological types (Figs. 11a, 12a), but have a restricted HFSE ratios falling into the field of quartz diorite (Fig. 11b).

2) They are mainly magnesian, and metaluminous and evolve to moderately peraluminous variety, consisting with I-type granitoids (Fig. 12b, c).

3) These granitoids show strongly LREE enriched, HREE depleted patterns without notable Eu anomalies (Fig. 13a), and display pronounced negative Nb, Ta, and Ti anomalies with either negative or positive Zr and Hf anomalies (Fig. 13b).

4) They show typical adakite-like Sr/Y and La/Yb ratios (Fig. 14a), falling into the field of volcanic-arc granitoids (Fig. 14b).

5) They may have formed in a post-collision extensional setting as a result of the upwelling of asthenospheric mantle due to the rollback of the subducting slab. This would trigger the upward migration of auriferous fluids from the lower crust or upper lithosphere mantle along deep fault(s) (e.g., Johnson shear zone) and precipitate in favourable sites (e.g., structural-chemical traps) in the middle to upper crust.

Fig. 9 Unit 6 Sickle group sandstone and polymictic conglomerate: **a)** quartz pebbly arkosic sandstone; **b)** poorly sorted, polymictic cobble conglomerate with wacke matrix and variously shaped clasts consisting of granitoid, vein quartz, banded iron formation, chert and felsic and mafic volcanic rocks, together with a few irregular felsic boulder-sized clasts; **c)** weakly foliated, matrix- to clast-supported, poorly sorted, polymictic pebble to cobble conglomerate with sandy matrix; and **d)** strongly foliated polymictic conglomerate with stretched granitoid, rhyolite, chert and banded iron formation clasts and subrounded quartz clasts, aligned along S_2 foliation planes that transposed S_0 bedding.

Fig. 10 Units 7, 8 and 9 rocks in the Gemmell Lake area: **a)** weakly foliated, massive, coarse-grained quartz diorite (subunit 7a); **b)** massive quartz-feldspar porphyry with up to 2% euhedral to subhedral magnetite (up to 3 mm) phenocrysts (unit 8); **c)** dacitic to rhyolitic mylonite showing brittle-ductile fabrics (S_2) and shear bands (unit 9); **d)** S-C fabric indicative of sinistral shear in felsic protomylonite with boudinaged quartz in dominant S_2 plane that cuts shallowly dipping S_1 fabrics (unit 9); **e)** silicified mafic mylonite cut by numerous quartz veins along a subvertical shear zone; dextral shear sense indicated by the asymmetric sigmoid quartz at the bottom of the photo (unit 9); **f)** quartz vein (~30 cm in width as shown by inset photo in lower right corner) containing megacrystic euhedral garnet crystals, which was emplaced along the contact between sheared unit 1 dacitic to rhyolitic rock and unit 2 basalt.